

Reducing the Cost of Quantum Chemical Data By Backpropagating Through Density Functional Theory

Alexander Mathiasen¹ Hatem Helal¹ Paul Balanca¹ Adam Krzywaniak¹ Ali Parviz² Frederik Hvilshøj
Blazej Banaszewski¹ Carlo Luschi¹ Andrew William Fitzgibbon¹

Abstract

Density Functional Theory (DFT) accurately predicts the quantum chemical properties of molecules, but scales as $O(N_{\text{electrons}}^3)$. Schütt et al. (2019) successfully approximate DFT 1000x faster with Neural Networks (NN). Arguably, the biggest problem one faces when scaling to larger molecules is the cost of DFT labels. For example, it took years to create the PCQ dataset (Nakata & Shimazaki, 2017) on which subsequent NNs are trained within a week. DFT labels molecules by minimizing energy $E(\cdot)$ as a “loss function.” We bypass dataset creation by directly training NNs with $E(\cdot)$ as a loss function. For comparison, Schütt et al. (2019) spent 626 hours creating a dataset on which they trained their NN for 160h, for a total of 786h; our method achieves comparable performance within 31h.

1. Introduction

Density Functional Theory (DFT) accurately predicts the quantum mechanical properties of molecules given their atom types and atom positions, with applications in the design of drugs (Gundelach et al., 2021) and materials (Chanussot et al., 2021). Accurate DFT can be enormously compute-intensive, so effort has been devoted to train Neural Networks (NNs) to efficiently approximate DFT. However, the high computational cost of DFT means that it is prohibitive to generate enough data to unlock the full benefit of NN scaling laws (Kaplan et al., 2020; Merchant et al., 2023). The largest existing datasets contain no more than 10^9 examples, computed using a low resolution DFT (a minimal basis set) (Mathiasen et al., 2023). These dataset sizes are almost certainly insufficient to scale molecular NNs to the magnitude of Large Language Models (LLMs), with current models no larger than a billion parameters, often less than 10M (Unke et al., 2021; Yu et al., 2023b).

¹Graphcore ²Mila - Québec AI Institute.

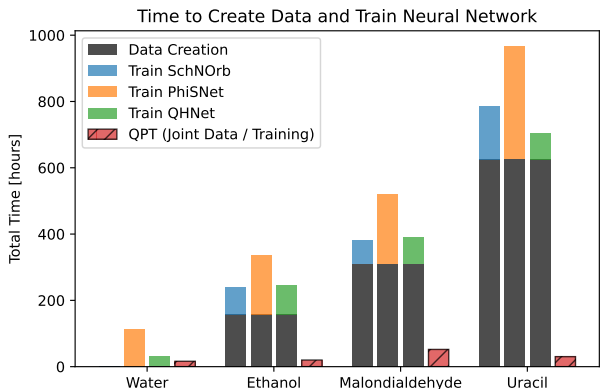


Figure 1. The time to label molecules with Density Functional Theory (DFT) scales as $O(N_{\text{electrons}}^3)$. The cubic scaling makes it impractical to create datasets with molecules like peptides or proteins with larger $N_{\text{electrons}}$. Our Quantum Pre-trained Transformer (QPT) bypasses the expensive DFT labeling by training with “DFT’s loss function”, the energy $E(\cdot)$. This circumvents the cost of creating datasets, paving a way to scale both the size of molecules and NNs.

We bypass the expensive DFT labeling by introducing a new pre-training technique. DFT labels molecules by minimizing the energy $E(\cdot)$ as a “loss function,” which require up to 50 DFT iterations to converge. Instead, we train our NN with $E(\cdot)$ as a loss function, which can be computed with 1 DFT iteration. Our Quantum Pre-trained Transformer (QPT) obtains comparable accuracy to prior work (Schütt et al., 2019; Unke et al., 2021; Yu et al., 2023b) on the Hamiltonian version of MD17, while eliminating the dataset creation cost (see Figure 1). Notably, the pre-training task is universal, in the sense that it allows one to compute any property that could be computed from DFT (e.g., forces, molecular orbital energies, homo-lumo gap, etc.). During training, it takes us 0.41s to compute and backpropagate through $E(\cdot)$, more than $200\times$ faster than the 88s Schütt et al. (2019) spent creating a training example (see Figure 3). This allows us to evaluate $E(X_i)$ on a new molecule X_i each step of training, generating an infinite stream of data, thereby mitigating overfitting and paving a way to arbitrarily scale model size.

Molecule	Data Creation	Train			Data Creation + Train			
		SchNOrb	PhisHNet	QHNet	SchNOrb	PhisHNet	QHNet	QPT
Water	-	-	112h	30h	-	-	-	16.3h
Ethanol	157h	82h	179h	90h	239h	356h	247h	20.1h
Malondialdehyde	309h	71h	210h	80h	380h	519h	389h	52.0h
Uracil	626h	160h	339h	79h	786h	965h	705h	30.2h

Table 1. Prior work (Schütt et al., 2019; Yu et al., 2023b) spends more time creating quantum data than training neural networks, e.g., Schütt et al. (2019) spent 626h creating the Uracil data but only trained for 160h. We drastically reduce the joint time to create data and train neural networks, while achieving comparable accuracy (see Table 2). We conjecture our approach will allow future work to arbitrarily scale the parameters of neural approximations to DFT.

1.1. Background and notation

The core of DFT is to compute the energy-minimizing electron configuration given a set of atoms $X = \{x_m\}_{m=1}^M$, where the m^{th} atom $x_m = (z_m, \mathbf{r}_m)$ is represented by its atomic number $z_m \in \mathbb{N}$ and atom position $\mathbf{r}_m \in \mathbb{R}^3$. The electron configuration or equivalently the density function, can be parameterized by the Hamiltonian H , in terms of which we define

$$\text{DFT}(X) := \min_H E(X; H), \quad (1)$$

where $E(X; H)$ is the energy of molecule X with electron configuration (density function) parameterized by H . It is common to represent $H \in \mathbb{R}^{N_{AO} \times N_{AO}}$ where N_{AO} is the number of (user specified) atomic orbitals. Following common practice, we use Gaussian Type Orbitals (GTOs) (Pople, 1999).

For many applications, the energy *per se* is not the quantity of interest, but the Hamiltonian itself

$$H^*(X) := \operatorname{argmin}_H E(X; H), \quad (2)$$

from which useful molecular properties can be derived. This motivated prior work (Schütt et al., 2019; Unke et al., 2021; Yu et al., 2023b) to train $\text{NN}(X; \theta)$ to approximate $H^*(X)$:

$$\text{NN}(X; \theta) \approx H^*(X) \quad (3)$$

Given a dataset of D molecules $\{X_i\}_{i=1}^D$, training consists of minimizing over the neural network parameters θ :

$$\theta^* = \operatorname{argmin}_\theta \sum_{i=1}^D |\text{NN}(X_i; \theta) - H^*(X_i)|_1 \quad (4)$$

where the labels $H^*(X_i)$ are precomputed with DFT (Khrabrov et al., 2022; Yu et al., 2023a).¹

In this paper, we are concerned with reducing the total time taken to train a new model, including dataset generation.

¹The loss, while written as a 1-norm, may be any loss function, e.g., Yu et al. (2023b) and Unke et al. (2021) use the sum of Mean Absolute Error (MAE) and Root Mean Squared Error (RMSE).

To see how we might find such a reduction, we insert the definition of $H^*(X)$ into the loss:

$$\theta^* = \operatorname{argmin}_\theta \sum_{i=1}^D \left| \text{NN}(X_i; \theta) - \underbrace{\operatorname{argmin}_H E(X_i, H)}_H \right|, \quad (5)$$

Takes 50 DFT iterations

Notably, each of the D optimization problems with respect to H can be solved in parallel:

$$H_1^*, \dots, H_D^* = \operatorname{argmin}_{H_1, \dots, H_D} \sum_{i=1}^D E(X_i; H_i). \quad (6)$$

Instead of learning from the solutions to Equation (6), we propose to learn directly from $E(\cdot)$, i.e., while existing losses (4) encourage $\text{NN}(X, \theta)$ to “look like” H , we define a loss which encourages $\text{NN}(X, \theta)$ to “act like” H , which we call the *implicit DFT loss*:

$$\theta^* = \operatorname{argmin}_\theta \sum_{i=1}^D \underbrace{E(X_i, \text{NN}(X_i; \theta))}_H, \quad (7)$$

Takes 1 DFT iteration

which can be trained using conventional machine-learning optimizers, but at considerably lower cost, as the optimizations over H and θ are interleaved. By analogy with the performance of stochastic gradient descent, where weight updates are made over many small batches per epoch, this implicit DFT loss allows an optimal θ to be found with significantly less computation.

One may view the “implicit DFT loss” as unsupervised learning, in the sense that there are no labels y_i . That said, we remark that learning to approximate DFT is different to the normal machine learning framework. The goal of supervised learning (Abu-Mostafa et al., 2012) is to approximate an unknown target function $f : X \rightarrow Y$ given examples of the function $(x_i, f(x_i))$. With DFT, the function $f = \text{DFT}$ we seek to approximate is known, differentiable, and can be implemented efficiently on hardware accelerators. In this paper, we advocate using these properties to move beyond supervised learning.

Why train NN to approximate DFT? Why not just use the existing DFT libraries? Previous works explore different advantages. The simplest advantage is that NN can accurately approximate DFT 1000x faster (Schütt et al., 2019; Unke et al., 2021; Yu et al., 2023b), often attributed to the cubic $O(N_{AO}^3)$ scaling of DFT. Another answer, is that performance on small biological datasets appear to improve when training on large amounts of quantum data (Beaini et al., 2024). One might imagine a variant of AlphaFold (Jumper et al., 2021) with 10B parameters (instead of just 100M), pre-trained to predict the quantum chemical structure of proteins-ligand conformations, then subsequently fine-tuned on the 200k protein databank (Berman et al., 2003). Creating the dataset for such a pre-training run is prohibitive. We present a training technique which bypasses the cost of dataset creation.

Contributions.

- We bypass the expensive DFT labeling by training NN with $E(\cdot)$ as a loss function.
- We can generate a new training example each step of training. This paves a way to arbitrarily scale the size of molecular foundation models.
- We demonstrate a Transformer applied to molecules with “the fewest possible modifications,” (Dosovitskiy et al., 2021) achieve comparable performance to prior work by scaling to just 300M parameters.

2. Quantum Pre-trained Transformer

Inspired by ViT (Dosovitskiy et al., 2021) we apply a standard Transformer directly to molecules “with the fewest possible modifications.”

We want the Transformer to use DFT as a loss function while dealing with differently sized molecules. DFTs energy function $E(\cdot)$ takes a square matrix of size $N_{AO} \times N_{AO}$ as input. Our Transformer outputs a $N_{AO} \times N_{AO}$ matrix by using the final pre-softmax attention head $A \in \mathbb{R}^{L \times L}$ where L is the sequence length. We then tokenize the input molecule into atomic orbitals so $L = N_{AO}$. For example, Schütt et al. (2019), Unke et al. (2021) and Yu et al. (2023b) use the DFT option (basis set) def2-SVP, for which hydrogen and oxygen are represented with 5 and 14 atomic orbitals respectively, so we would have 5 hydrogen tokens H_1, \dots, H_5 and 14 oxygen tokens O_1, \dots, O_{14} ; this is visualized in Figure 2 within the box labeled “Tokenizer.” We translate the input positions r so it has mean $\mu(r) = 0$ and subsequently rotate it so it has a diagonal covariance matrix $\Sigma(rR) = \text{diag}(\sigma_{11}, \dots, \sigma_{NN})$ (not included in Figure 2 for simplicity). We then create a list of atomic orbital token indices $\hat{z} \in \mathbb{Z}^m$ and $\hat{r} \in \mathbb{R}^{m \times 3}$ where m is the total number

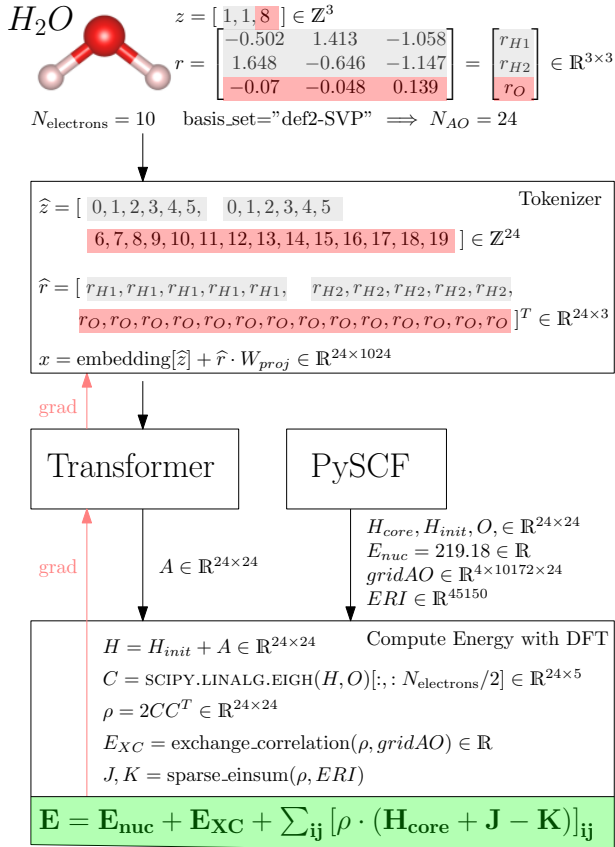


Figure 2. Visualization of how a molecule gets tokenized so our Transformer can process it and output an appropriately shaped matrix for the DFT energy computation.

of atomic orbitals used to represent the input molecule (e.g. 24 for H_2O used as an example in Figure 2). The input $x = \text{embedding}[\hat{z}] + \hat{r} \cdot W_{proj} \in \mathbb{R}^{m \times d_{model}}$ is passed to a vanilla Transformer Encoder (Vaswani et al., 2017). Since we use the final layer’s attention matrix A for prediction, we employ a single attention head and set $Q = K$ so the output A is symmetric, $A = A^T$.

We use $H = H_{init} + A$ to compute energy $E(\cdot)$ as illustrated in Figure 2 within the box labeled “Compute Energy with DFT” in Figure 2). We precompute the necessary DFT tensors using the DFT library PySCF (Sun et al., 2018) on the CPU asynchronously in a PyTorch dataloader.

Using an Initial DFT Guess. DFT libraries like PySCF speed up convergence by using an initial guess for the density matrix ρ . Specifically, PySCF (Sun et al., 2018) uses the “minao initialisation” ρ_0 (Almlöf et al., 1982; Van Lenthe et al., 2006). We incorporate this initial guess to our Transformer by using $H_{init} = H(\rho_0)$ where $H(\rho_0)$ is the Hamiltonian computed from ρ_0 using Roothaan’s equation (Roothaan, 1951). We found this to improve optimization convergence.

Quantum Biased Attention. Inspired by Transformer-M (Luo et al., 2023), we bias the (non-output) pre-softmax attention matrices by all pairs of dot products $P_{ij} = \hat{r}_i^T \hat{r}_j$ and six cheap-to-compute DFT matrices $H_{core}, L^{-1}H_{core}L^{-1^T}, \rho_0, (J - K/2), V_{xc}, H(\rho_0)$.² Our Transformer has $n_{heads} = 16$ and we apply each DFT matrix to 2 different attention heads, so the first 14 heads are biased and the remaining 2 are “free.”

Density Mixing. We found using the DFT technique “density mixing” to compute $E(\cdot)$ improved performance. Figure 2 shows the content of a DFT iteration inside the “Compute Energy” box. Density mixing changes this to:

$$\rho = \alpha\rho + (1 - \alpha)2CC^T \quad \alpha \in [0, 1).$$

We like to think of density mixing as a residual connection and choose $\alpha = 0.5$. Density mixing may break the idempotency $\rho^2 = \rho$ needed to compute $E(\cdot)$. We fix this by running yet another DFT iteration. In summary, our method use one DFT to initialize $H(\rho_0)$ followed by another three DFT iterations to stably compute $E(\cdot)$. One might thus view QPT as a hybrid ML/DFT method, with a NN sandwiched between an initial DFT iteration followed by three refining DFT iterations, all trained by backpropagating through DFT.

3. Experiments

The goal of this section is to demonstrate that QPT can achieve comparable performance to prior work while bypassing the cost of DFT dataset creation. We compare QPT to Schütt et al. (2019), Unke et al. (2021) and Yu et al. (2023b), which train neural networks to predict the Hamiltonian matrix using supervised learning, i.e., each example consists of $(X_i, H^*(X_i))$ as in Equation (4). They train a separate neural network on four different molecules $X = \{\text{water, ethanol, malondialdehyde, uracil}\}$ with training sets of sizes $\{500, 25k, 25k, 25k\}$. We also train one QPT for each molecule, but use the “implicit DFT loss” Equation (7) computing $E(\cdot)$ on the fly (i.e., we never use the precomputed labels $H^*(X_i)$). In Table 1, we compare the dataset creation time next to neural network training time, as reported in prior work (Schütt et al., 2019; Unke et al., 2021; Yu et al., 2023b).

We trained a 302M QPT to minimize Equation (7) using the same X_i as Schütt et al. (2019) without using the labels $H(X_i)$. This requires a differentiable implementation of $E(\cdot)$. Our implementation is based on Mathiasen et al. (2023) and thus use def2-SVP/B3LYP instead of def2-

²The matrix $L^{-1}H_{core}L^{-1^T}$ appear in DFT when translating the generalized eigenproblem `SCIPY.LINALG.EIGH(H_{core}, O)` into an eigenproblem `NP.LINALG.EIGH($L^{-1}H_{core}L^{-1^T}$)` by using $L = \text{NP.LINALG.CHOLESKY}(O)$.

SVP/PBE as done in Schütt et al. (2019).³ After training QPT no more than 52h on a single hardware accelerator, it achieved comparable accuracy to prior work (see Table 2). For example: on Uracil, QPT took 31h to train compared to 626+160h=786h for SchNOrb. Notably, the Mean Absolute Error (MAE) of QPT relative to PySCF was 0.524meV for energy E , 39.46 μ Ha for Hamiltonian H and 409.21 μ Ha for molecular orbital energies ϵ . This is comparable to prior works, i.e., slightly better (lower) than SchNorb and slightly worse (larger) than QHNet and PhiSNet. Notably, QPT is never given any labels during training, its predictions are inferred by optimizing $E(\cdot)$ (just like DFT). QPT performed worst on malondialdehyde, even though we trained it for longer and added another density-mixed DFT iteration.

Training Details. On all tasks, we trained a 302M Transformer following “GPT medium” as closely as possible, i.e., $d_{model} = 1024, n_{heads} = 16, n_{layers} = 24$. We used the Adam optimizer (Kingma & Ba, 2014) with $\beta_1 = 0.9, \beta_2 = 0.95, 0.1$ weight decay and the LR schedule from minGPT with 100 warmup steps, $lr = 10^{-4}/16/\sqrt{5}$ decaying to $lr = 10^{-6}/16$ at step 200k. We use a batch size of 1. The DFT tensors needed to evaluate $E(\cdot)$ are prepared on the CPU using PySCF run in a PyTorch dataloader. Similar to how DFT has 50 iterations, we keep a window of the last 6-8 tensors to avoid throttling the dataloader.

Adjusting DFT Tolerance. The energy convergence threshold of PySCF is by default $2.72 \cdot 10^{-9}$ eV compared to the 10^{-4} eV error of SchNOrb. We suspect it is sufficient that the accuracy of $E(\cdot)$ is “only” $10\times$ better than the desired accuracy of our NN, e.g., if we want to train QPT on Uracil to 0.3 meV accuracy, it is okay that our DFT is 0.03 meV inaccurate. Prior to training, we ran PySCF to determine sufficiently accurate DFT options which minimize computational resources. For example: For Uracil we could reduce the exchange correlation grid level from 3 to 2, which reduced the DFT tensor “gridAO” from (4, 152320, 132) to (4, 111896, 132) (roughly 25% faster). We also introduce a threshold on the Electron Repulsion Integrals (ERIs) discarding anything below 10^{-7} , which reduced the number of distinct ERIs from 34.7M to 25.7M (roughly 25% faster). Finally, while $E(\cdot)$ was evaluated in float64, we evaluated NN in float32. Similar to how DFT implementations like TeraChem (Seritan et al., 2021) employ variable grid sizes between DFT iterations, we conjecture NNs trained with the implicit DFT loss can utilize adaptive grid sizes. This opens an interesting avenue for future research, exploring how the plethora of optimization techniques from DFT might translate to hybrid ML/DFT methods (DIIS, density mixing, minao initialization, ERI symmetries and sparsity, ...).

³B3LYP is more computationally demanding. It computes K from Figure 2 which PBE “skips.”

Dataset	Method	XC	ΔE [meV] ↓	ΔH [$10^{-6} E_h$] ↓	$\Delta \epsilon$ [$10^{-6} E_h$] ↓	Parameters [M] ↑
Water	SchNOorb	PBE	1.435	165.37	279.3	-
	PhiSNet	PBE	-	7.87	29.81	3.839M
	QHNet	PBE	-	10.49	31.62	2.419M
	QPT (ours)	B3LYP	0.052	38.06	202.03	302M
Ethanol	SchNOorb	PBE	0.361	187.4	334.4	-
	PhiSNet	PBE	-	19.60	101.10	8.673M
	QHNet	PBE	-	20.45	81.29	3.917M
	QPT (ours)	B3LYP	0.073	18.49	148.90	302M
Malondialdehyde	SchNOorb	PBE	0.353	191.1	400.6	-
	PhiSNet	PBE	-	21.89	104.76	8.869M
	QHNet	PBE	-	22.07	86.04	3.925M
	QPT (ours)	B3LYP	2.006	81.29	697.43	302M
Uracil	SchNOorb	PBE	0.848	227.8	1760	93M
	PhiSNet	PBE	-	18.89	146.14	9.135M
	QHNet	PBE	-	20.33	113.48	4.049M
	QPT (ours)	B3LYP	0.524	39.46	409.21	302M

Table 2. Validation error of different molecules. Schütt et al. (2019) used def2-SVP/PBE, we used def-SVP/B3LYP to make $E(\cdot)$ differentiable. We measure the mean absolute error (MAE) between DFT and NN for energy E , Hamiltonian H and molecular orbital energies ϵ . Notably, QPT obtain comparable performance than prior work, while bypassing the huge cost to precompute datasets.

Comparing Training Speed to Data Generation In Figure 3, we compare the time to label a training example as reported in prior work⁴, compared to the time to compute and backpropagate through QPT with the “implicit DFT loss.” The time to perform a DFT computation scales with the cube of the number of atomic orbitals $O(N_{AO}^3)$. Using DFT to compute the energy loss $E(\cdot)$ amounts to a few DFT iterations and thus also scale $O(N_{AO}^3)$ (backpropagation takes only a constant amount of time longer). In practice, we found the time to evaluate and backpropagate through $E(\cdot)$ is around $200\times$ faster than creating a training example by running DFT as reported by prior work. This reduction seem to arise from several factors: fewer DFT iterations, hardware acceleration, lower DFT accuracy tuned to NN, efficient JAX sparse matmul implementation, pre-computing DFT tensors asynchronously on the CPU in the PyTorch dataloader.

Adjusting DFT Iterations. Early in training, we used a single DFT iteration to compute $E(\cdot)$ as in Figure 2. We add an additional iteration with density mixing after 150k steps, before the learning rate scheduler finishes. We add a final DFT iteration for validation to ensure idempotency of the density matrix $\rho^2 = \rho$. The training speed numbers reported in Figure 3 assume the worst case, i.e., four DFT iterations. To our surprise, using four DFT iterations throughout training performed worse than incrementally adding the DFT iterations.

⁴The numbers in Unke et al. (2021) used an old 32nm CPU Intel Xeon E5-2690. We also report numbers on our 7nm AMD EPYC 7542 with PySCF in def2-SVP/B3LYP with default options.

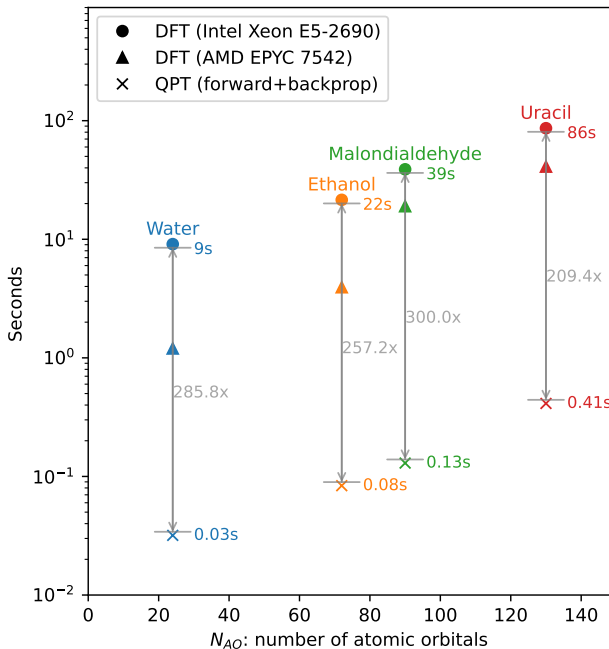


Figure 3. Time to label a training example using DFT as reported by Schütt et al. (2019), Unke et al. (2021) and Yu et al. (2023b), compared to a forward/backward pass of QPT using energy $E(\cdot)$ as a loss function. Bypassing the expensive labeling gives us the ability to evaluate $E(\cdot)$ on a new X_i each iteration. Triangle is time of DFT using our newer CPUs.

Molecule	DFT				NN			DFT/NN hybrid QPT
	SchNOrb	PhiSNet	QHNet	Us	SchNOrb	PhiSNet	QHNet	
Water	9.10s	-	11.38s	1.2s	0.033s	-	0.0109s	0.011s (0.050s)
Ethanol	22.2s	21.6s	25.1s	3.9s	0.033s	0.027s	0.0711s	0.040s (0.365s)
Malondialdehyde	43.6s	38.9s	40.6s	19s	0.034s	0.029s	0.0792s	0.065s (0.853s)
Uracil	88.4s	86.6s	-	41s	0.038s	0.050s	-	0.188s (1.729s)

Table 3. Inference numbers. We report numbers “ $xs (ys)$ ” where x is the time for an inference of QPT and its DFT iterations, while ys is the total time which includes preparing DFT tensors in our dataloader. The time to prepare the DFT tensors take $10\times$ longer than running QPT and the DFT iterations. We can hide this during training by keeping a window of the last 6-8 molecules, however, this is not possible during inference.

Inference Speed. We compare the inference time of QPT against DFT and previous NNs in Table 3. We report both the inference time due to QPT (including its DFT iterations) and total time including the dataloader preparing DFT tensors. The dataloader increase time consumption almost $10\times$, e.g., from 0.188s to 1.729s for Uracil. During training, we mitigated this issue by keeping the last 6 to 8 molecules in RAM and repeating training on them 6-8 times. This is not possible during inference (each molecule is seen only once).

Loss curves. Figure 5 plots the error of a single ethanol validation molecule as training QPT progress. From left: The first plot visualises the energy computed by DFT DFT_E as a horizontal line, and how the energy predicted by QPT QPT_E gets closer as training progress. As the lines get closer it becomes hard to see their difference, so the next plot instead visualises their absolute difference $|DFT_E - QPT_E|$. We similarly plot the mean absolute error (MAE) of the validation molecule for the Hamiltonian matrix, and the molecular orbital energies computed as the eigenvalues from the generalized eigenproblem `SCIPY.LINALG.EIGH(H, O)`.

Preliminary Scaling to Peptides. As a preliminary proof-of-concept for proteins/peptides, we trained a QPT on different conformations of alanine dipeptide, represented by two angles (ϕ, ψ) (see Figure 4). During training, we create random conformations by picking two angles (ϕ, ψ) uniformly at random from $[0, 180]^2$. We then measure validation performance within $[0, 180]^2$ and extrapolation performance on angles not seen during training (i.e. $[0, 360]^2 \setminus [0, 180]^2$). Since each conformation is represented by a 2d point (ϕ, ψ) , we can visualize the error $\log |DFT_E(\phi, \psi) - QPT_E(\phi, \psi)|$ in a 2d coordinate system (see Figure 4). The model exhibits minor extrapolation; the error within $[0, 200]^2 \setminus [0, 180]^2$ is similar to the error within the training distribution $[0, 180]^2$. To speed up experimentation we use the less accurate DFT options STO3G/B3LYP as done in (Mathiasen et al., 2023). This QPT experiment did not include the quantum biased attention and the minao initialization; we expect re-training with these techniques would improve performance.

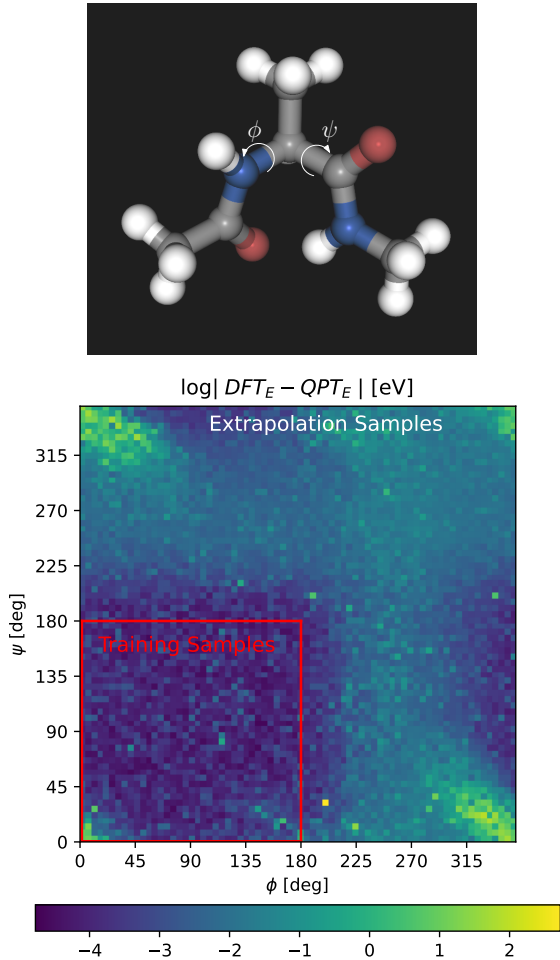


Figure 4. Comparison of the models performance on conformations inside the training distribution $(\phi, \psi) \in [0, 180]^2$ relative to the performance outside the training distribution $(\phi, \psi) \in [0, 360]^2 \setminus [0, 180]^2$. The model exhibits minor extrapolation to angles $[180, 200]$ not seen during training. A typical energy value is around 13000eV, so an error $\log(|DFT_E - QPT_E|) = -4$ could mean that the neural network predicted 13000.0001 instead of 13000.0000. Chemical accuracy is 0.040eV).

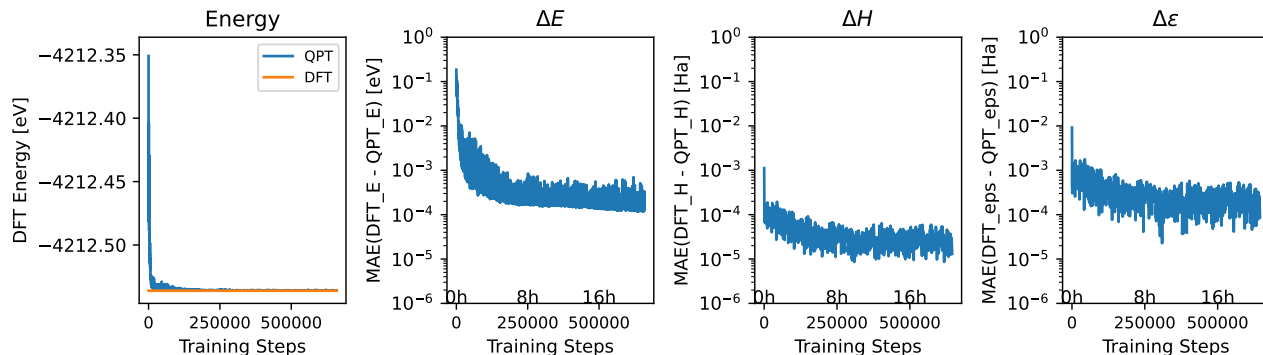


Figure 5. On the left, we visualize QPT_E during training on a single validation example, for which we also computed DFT_E . Next, we visualize their difference ΔE . We finally present a similar plot for the resulting Hamiltonian H and its molecular orbital energies ϵ .

4. Limitations and Future Work

DFT options. Our main experiments demonstrate QPT with the implicit DFT loss can achieve error relative to def2-SVP/B3LYP that, in absolute value, is similar to the error QHNet/SchNOrb/PhiSNet achieve relative to def2-SVP/PBE. While the def2-SVP/B3LYP options have been used by related work (Yu et al., 2023a), the differences between the PBE and B3LYP functionals are significant.⁵ The B3LYP functional is more computationally intense since it requires computing the exact Hartree-Fock exchange (the K matrix in Figure 2). We estimate using PBE would halve our training time, since roughly 45% of the training time was spent computing K .

Inference Speed. Our inference speed is currently 10x to 50x worse than prior work. The main issue lies in the precomputation of DFT tensors. It turns out the most of this time is spent preparing indices for the sparse einsum, not computing the actual DFT tensors (integrals, XC grids, etc). We estimate fixing the issue will improve inference time 5x.

Generating New Data. The implicit DFT loss allows us to evaluate $E(\cdot)$ on a new X_i every step of training. Never seeing the same training example, as is sometimes the case for Large Language Models, practically solves overfitting. In our Table 2 experiments, we did not use this ability. The reason is that the benchmark data has a particular distribution of X_i 's which we were unable to reproduce. When scaling to large pre-training runs with billions of parameters and hundreds of hardware accelerators, we expect controlling the generation of X_i will be of immense importance.

Inductive Bias. This work demonstrate a simple QPT architecture without inductive biases can obtain comparable

⁵An excellent overview covering the taxonomy of different functionals can be found in (Rappoport et al., 2006)

performance to prior work. It remains to be shown whether inductive biases can improve the performance of models trained with the “implicit DFT loss.” We find it particularly interesting whether inductive biases improve or worsen potential scaling laws.

Scaling to Protein-ligands. We tested our current implementation for molecules no larger than $N_{AO} = 132$. This is very small compared to protein-ligand interactions which contain around 4000 atoms, i.e. $N_{AO} < 20k$ in STO3G or $N_{ao} < 52k$ in def2-SVP. Scaling to this size presents a formidable challenge. In our alanine dipeptide we experimenting with a batching technique. While we found no computational benefits at the scale of the dipeptide, we conjecture its benefit will improve at protein-scale. The idea is to create a batch of similar molecules: fix the protein ($N_{AO} = 19900$) and create 200 training examples by moving only the ligand ($N_{AO} = 100$). To prepare the DFT tensors for the batch with 200 examples, we only need to compute the interactions within the proteins atomic orbitals once; the cost of preparing such 200 training examples is therefore almost the same as preparing 1 protein.⁶

5. Related Work

5.1. Supervised Neural Approximations to DFT

A large body of prior work train neural networks to approximate outputs of DFT (Unke et al., 2021; Yu et al., 2023b;a; Schütt et al., 2019; 2018; Batatia et al., 2022). Some train their NN to predict the Hamiltonian matrix (Unke et al., 2021; Yu et al., 2023b; Schütt et al., 2019), others train to predict properties like homo-lumo gap (Schütt et al., 2018; Masters et al., 2023) while yet others learn to approximate forces (Batatia et al., 2022; Batzner et al., 2022). Notably,

⁶One can augment moving the ligand with changing the atom types $C \leftrightarrow O$ and $N \leftrightarrow F$.

while it may be faster to directly predict quantities like forces, both homo-lumo gap and forces can be derived from the Hamiltonian. This line of work differs to ours, in that they all train neural networks with supervised learning using datasets with precomputed labels. We instead propose to use $E(\cdot)$ as a loss function.

The need for labeled datasets has sparked a large amount of previous work creating public datasets: QM9 (Ramakrishnan et al., 2014), ANI1x (Smith et al., 2020), Hamiltonian MD17 (Schütt et al., 2019), PCQ (Nakata & Shimazaki, 2017), OpenCatalyst (Chanussot et al., 2021), QM1B (Mathiasen et al., 2023), nablaDFT (Khrabrov et al., 2022) and many more. The time to compute these datasets can be very huge, for example, it took a reported 2 years to generate the PCQ dataset (Nakata & Shimazaki, 2017). Furthermore, for datasets that store DFT matrices, data storage also becomes burdensome, e.g., nablaDFT contains 1M molecules and consumes 7TB of storage. This storage requirement is circumvented when training with the implicit DFT loss (note that a 1M protein dataset with $N_{AO} = 50k$ would take up 20PB in float64).

Finally, the majority of prior work focus on either dataset creation or neural network training. Our work differs, in that we join the optimization involved in data creation and neural network training. This opens interesting new avenues of merging prior DFT optimization techniques, specifically, tailoring the DFT optimization to neural network pre-training. We preliminarily explored adjusting the DFT accuracy by changing the XC grid size, the electron repulsion threshold and the number of DFT iterations used to compute $E(\cdot)$.

5.2. Differentiable DFT

The usual DFT algorithm relies on evaluating several derivatives. Most DFT libraries implement derivatives manually instead of using automatic differentiation. This is in contrast with the approach adopted in machine learning where frameworks such as PyTorch (Paszke et al., 2019), Jax (Bradbury et al., 2018), and Tensorflow (Abadi et al., 2015) provide powerful automatic differentiation capabilities. This has motivated a line of work which reimplement DFT within modern machine learning libraries, allowing automatic differentiation, and, in certain cases, even hardware acceleration (Li et al., 2020; Zhang & Chan, 2022; Kasim & Vinko, 2021; Mathiasen et al., 2023; Li et al., 2023).

Notably, Li et al. (2020), Kasim & Vinko (2021) and Casares et al. (2023) use their differentiable DFT to improve the accuracy of DFT by training a neural exchange correlation functional by backpropagating through DFT. Our work differs, in that we do not train exchange correlation functionals to improve the accuracy of DFT. Instead, we use a differentiable DFT implementation of $E(\cdot)$ to interleave the optimization of neural network and DFT

$$\min_{\theta} \sum_{i=1}^D E(X_i, \text{NN}(X_i, \theta)).$$

Zhang & Chan (2022) introduced a plugin to PySCF which provides automatic differentiation by replacing NumPy (Harris et al., 2020) with the compatible `jax.numpy` (Bradbury et al., 2018) modules, however, they remain reliant on libcint and libxc so do not support hardware acceleration. Mathiasen et al. (2023) introduced a small subset of PySCF with hardware acceleration, and, sufficient automatic differentiation for our use-case, i.e., we can compute $\nabla_H E(H)$. This led us to base our implementation of Mathiasen et al. (2023).

Li et al. (2023) revisited DFT from a modern deep learning perspective. In particular, they demonstrate that the DFT optimization problem $\min_{M_i} E(X_i, M_i)$ can be minimized using Gradient Descent with the Adam optimizer. One might view our work as a continuation of their work. Instead of optimizing $\min_{H_i} E(X_i, H_i)$ with respect to one matrix H_i for each molecule X_i , we optimize neural network parameters ϕ for many molecules $\min_{\theta} \sum_{i=1}^D E(X_i, \text{NN}(X_i, \theta))$. We then compare the resulting neural network NN against those trained with supervised learning (Schütt et al., 2019; Unke et al., 2021; Yu et al., 2023b).

6. Conclusion

Prior work spend more time labeling datasets with DFT than subsequent NN training. For example, it took years to create the PCQ dataset (Nakata & Shimazaki, 2017) on which NNs are usually trained within a week. We demonstrated training QPT with “DFTs loss function” yields comparable accuracy to prior work (Table 2), while mitigating the huge dataset creation cost (Table 1). For example, on the Uracil dataset, QPT achieved comparable accuracy to SchNOrb within 31h, whereas SchNOrb was trained for 160h on a dataset which took 626h to create (i.e. a total of 786h).

References

- Abadi, M., Agarwal, A., Barham, P., Brevdo, E., Chen, Z., Citro, C., Corrado, G. S., Davis, A., Dean, J., Devin, M., Ghemawat, S., Goodfellow, I., Harp, A., Irving, G., Isard, M., Jia, Y., Jozefowicz, R., Kaiser, L., Kudlur, M., Levenberg, J., Mané, D., Monga, R., Moore, S., Murray, D., Olah, C., Schuster, M., Shlens, J., Steiner, B., Sutskever, I., Talwar, K., Tucker, P., Vanhoucke, V., Vasudevan, V., Viégas, F., Vinyals, O., Warden, P., Wattenberg, M., Wicke, M., Yu, Y., and Zheng, X. TensorFlow: Large-Scale Machine Learning on Heterogeneous Systems, 2015.
- Abu-Mostafa, Y. S., Magdon-Ismail, M., and Lin, H.-T. Learning From Data. 2012.
- Almlöf, J., Fægri Jr, K., and Korsell, K. Principles for a Direct SCF Approach to LICAO–MOab-*initio* Calculations. Journal of Computational Chemistry, 1982.
- Batatia, I., Kov’acs, D. P., Simm, G. N. C., Ortner, C., and Csányi, G. MACE: Higher Order Equivariant Message Passing Neural Networks for Fast and Accurate Force Fields. NeurIPS, 2022.
- Batzner, S., Musaelian, A., Sun, L., Geiger, M., Mailoa, J. P., Kornbluth, M., Molinari, N., Smidt, T. E., and Kozinsky, B. E(3)-Equivariant Graph Neural Networks for Data-Efficient and Accurate Interatomic Potentials. Nature communications, 2022.
- Beaini, D., Huang, S., Cunha, J. A., Moisescu-Pareja, G., Dymov, O., Maddrell-Mander, S., McLean, C., Wenkel, F., Müller, L., Mohamud, J. H., et al. Towards Foundational Models for Molecular Learning on Large-Scale Multi-Task Datasets. ICLR, 2024.
- Berman, H., Henrick, K., and Nakamura, H. Announcing the Worldwide Protein Data Bank. Nature structural & molecular biology, 2003.
- Bradbury, J., Frostig, R., Hawkins, P., Johnson, M. J., Leary, C., Maclaurin, D., Necula, G., Paszke, A., VanderPlas, J., Wanderman-Milne, S., and Zhang, Q. JAX: Composable Transformations of Python+NumPy Programs, 2018.
- Casares, P. A., Baker, J. S., Medvidovic, M., Reis, R. d., and Arrazola, J. M. Grad DFT: A Software Library for Machine Learning Enhanced Density Functional Theory. arXiv preprint arXiv:2309.15127, 2023.
- Chanussot, L., Das, A., Goyal, S., Lavril, T., Shuaibi, M., Riviere, M., Tran, K., Heras-Domingo, J., Ho, C., Hu, W., et al. Open Catalyst 2020 (OC20) Dataset and Community Challenges. Acs Catalysis, 2021.
- Dosovitskiy, A., Beyer, L., Kolesnikov, A., Weissenborn, D., Zhai, X., Unterthiner, T., Dehghani, M., Minderer, M., Heigold, G., Gelly, S., Uszkoreit, J., and Houslyby, N. An Image is Worth 16x16 Words: Transformers for Image Recognition at Scale. In ICLR, 2021.
- Gundelach, L., Fox, T., Tautermann, C. S., and Skylaris, C.-K. Protein–Ligand Free Energies of Binding From Full-Protein DFT Calculations: Convergence and Choice of Exchange–Correlation Functional. Physical Chemistry Chemical Physics, 2021.
- Harris, C. R., Millman, K. J., van der Walt, S. J., Gommers, R., Virtanen, P., Cournapeau, D., Wieser, E., Taylor, J., Berg, S., Smith, N. J., Kern, R., Picus, M., Hoyer, S., van Kerkwijk, M. H., Brett, M., Haldane, A., del Río, J. F., Wiebe, M., Peterson, P., Gérard-Marchant, P., Sheppard, K., Reddy, T., Weckesser, W., Abbasi, H., Gohlke, C., and Oliphant, T. E. Array Programming with NumPy. Nature, 2020.
- Jumper, J., Evans, R., Pritzel, A., Green, T., Figurnov, M., Ronneberger, O., Tunyasuvunakool, K., Bates, R., Žídek, A., Potapenko, A., et al. Highly Accurate Protein Structure Prediction with AlphaFold. Nature, 2021.
- Kaplan, J., McCandlish, S., Henighan, T., Brown, T. B., Chess, B., Child, R., Gray, S., Radford, A., Wu, J., and Amodei, D. Scaling Laws for Neural Language Models. arXiv preprint arXiv:2001.08361, 2020.
- Kasim, M. F. and Vinko, S. M. Learning the Exchange–Correlation Functional from Nature with Fully Differentiable Density Functional Theory. Physical Review Letters, 2021.
- Khrabrov, K., Shenbin, I., Ryabov, A., Tsybin, A., Telepov, A., Alekseev, A., Grishin, A., Strashnov, P., Zhilyaev, P., Nikolenko, S., et al. nDFT: Large-Scale Conformational Energy and Hamiltonian Prediction Benchmark and Dataset. Physical Chemistry Chemical Physics, 2022.
- Kingma, D. P. and Ba, J. Adam: A Method for Stochastic Optimization. arXiv preprint arXiv:1412.6980, 2014.
- Li, L., Hoyer, S., Pederson, R., Sun, R., Cubuk, E. D., Riley, P. F., and Burke, K. Kohn-Sham Equations as Regularizer: Building prior Knowledge Into Machine-Learned Physics. Physical Review Letters, 2020.
- Li, T., Lin, M., Hu, Z., Zheng, K., Vignale, G., Kawaguchi, K., Neto, A. C., Novoselov, K. S., and YAN, S. D4FT: A Deep Learning Approach to Kohn-Sham Density Functional Theory. In ICLR, 2023.
- Luo, S., Chen, T., Xu, Y., Zheng, S., Liu, T.-Y., Wang, L., and He, D. One Transformer Can Understand Both 2D & 3D Molecular Data. In ICLR, 2023.

- Masters, D., Dean, J., Klaeser, K., Li, Z., Maddrell-Mander, S., Sanders, A., Helal, H., Beker, D., Fitzgibbon, A. W., Huang, S., Rampásek, L., and Beaini, D. GPS++: Reviving the Art of Message Passing for Molecular Property Prediction. Transactions on Machine Learning Research, 2023.
- Mathiasen, A., Helal, H., Klaeser, K., Balanca, P., Dean, J., Luschi, C., Beaini, D., Fitzgibbon, A. W., and Masters, D. Generating QM1B with PySCF_{IPU}. In NeurIPS - Datasets and Benchmarks Track, 2023.
- Merchant, A., Batzner, S., Schoenholz, S. S., Aykol, M., Cheon, G., and Cubuk, E. D. Scaling Deep Learning for Materials Discovery. Nature, 2023.
- Nakata, M. and Shimazaki, T. PubChemQC Project: A Large-Scale First-Principles Electronic Structure Database for Data-Driven Chemistry. Journal of Chemical Information and Modeling, 2017.
- Paszke, A., Gross, S., Massa, F., Lerer, A., Bradbury, J., Chanan, G., Killeen, T., Lin, Z., Gimelshein, N., Antiga, L., et al. Pytorch: An Imperative Style, High-Performance Deep Learning Library. NeurIPS, 2019.
- Pople, J. A. Nobel Lecture: Quantum Chemical Models. Reviews of Modern Physics, 1999.
- Ramakrishnan, R., Dral, P. O., Rupp, M., and Von Lilienfeld, O. A. Quantum Chemistry Structures and Properties of 134 Kilo Molecules. Scientific data, 2014.
- Rappoport, D., Crawford, N. R., Furche, F., and Burke, K. Approximate Density Functionals: Which Should I Choose? Encyclopedia of Inorganic Chemistry, 2006.
- Roothaan, C. C. J. New Developments in Molecular Orbital Theory. Reviews of modern physics, 1951.
- Schütt, K. T., Sauceda, H. E., Kindermans, P.-J., Tkatchenko, A., and Müller, K.-R. Schnet-A Deep Learning Architecture for Molecules and Materials. The Journal of Chemical Physics, 2018.
- Schütt, K. T., Gastegger, M., Tkatchenko, A., Müller, K.-R., and Maurer, R. J. Unifying Machine Learning and Quantum Chemistry with a Deep Neural Network for Molecular Wavefunctions. Nature communications, 2019.
- Seritan, S., Bannwarth, C., Fales, B. S., Hohenstein, E. G., Isborn, C. M., Kokkila-Schumacher, S. I. L., Li, X., Liu, F., Luehr, N., Snyder Jr., J. W., Song, C., Titov, A. V., Ufimtsev, I. S., Wang, L.-P., and Martínez, T. J. TeraChem: A Graphical Processing Unit-Accelerated Electronic Structure Package for Large-Scale AB Initio Molecular Dynamics. WIREs Computational Molecular Science, 2021.
- Smith, J. S., Zubatyuk, R., Nebgen, B., Lubbers, N., Barros, K., Roitberg, A. E., Isayev, O., and Tretiak, S. The ANI-1ccx and ANI-1x Data Sets, Coupled-Cluster and Density Functional Theory Properties for Molecules. Scientific Data, 2020.
- Sun, Q., Berkelbach, T. C., Blunt, N. S., Booth, G. H., Guo, S., Li, Z., Liu, J., McClain, J. D., Sayfutyarova, E. R., Sharma, S., et al. PySCF: the Python-Based Simulations of Chemistry Framework. Wiley Interdisciplinary Reviews: Computational Molecular Science, 2018.
- Unke, O., Bogojeski, M., Gastegger, M., Geiger, M., Smidt, T., and Müller, K.-R. SE (3)-equivariant prediction of molecular wavefunctions and electronic densities. Advances in Neural Information Processing Systems, 2021.
- Van Lenthe, J., Zwaans, R., Van Dam, H. J., and Guest, M. Starting SCF Calculations By Superposition of Atomic Densities. Journal of Computational Chemistry, 2006.
- Vaswani, A., Shazeer, N., Parmar, N., Uszkoreit, J., Jones, L., Gomez, A. N., Kaiser, Ł., and Polosukhin, I. Attention Is All You Need. NeurIPS, 2017.
- Yu, H., Liu, M., Luo, Y., Strasser, A., Qian, X., Qian, X., and Ji, S. QH9: A Quantum Hamiltonian Prediction Benchmark for QM9 Molecules. In NeurIPS, 2023a.
- Yu, H., Xu, Z., Qian, X., Qian, X., and Ji, S. Efficient and Equivariant Graph Networks for Predicting Quantum Hamiltonian. In Krause, A., Brunskill, E., Cho, K., Engelhardt, B., Sabato, S., and Scarlett, J. (eds.), ICML, 2023b.
- Zhang, X. and Chan, G. K.-L. Differentiable Quantum Chemistry with PySCF for Molecules and Materials at the Mean-Field Level and Beyond. The Journal of Chemical Physics, 2022.